

Preprint of article to appear in *Atmospheric Environment*:
Development of algorithms and approximations for
rapid operational air quality modelling

Steven R. H. Barrett*, Rex E. Britter

*Department of Engineering and Institute for Aviation and the Environment,
University of Cambridge, Trumpington Street, Cambridge CB2 1PZ, UK*

Abstract

In regulatory and public health contexts the long-term average pollutant concentration in the vicinity of a source is frequently of interest. Well-developed modelling tools such as AERMOD and ADMS are able to generate time-series air quality estimates of considerable accuracy, applying an up-to-date understanding of atmospheric boundary layer behaviour. However, such models incur a significant computational cost with runtimes of hours to days. These approaches are often acceptable when considering a single industrial complex, but for widespread policy analyses the computational cost rapidly becomes intractable. In this paper we present some mathematical techniques and algorithmic approaches that can make air quality estimates several orders of magnitude faster. We show that, for long-term average concentrations, lateral dispersion need not be accounted for explicitly. This is applied to a simple reference case of a ground-level point source in a neutral boundary layer. A scaling law is also developed for the area in exceedance of a regulatory limit value.

Key words: Local air quality, Dispersion modelling, Long-term average concentrations, Point sources

1. Introduction

Operational dispersion modelling on the local scale (~ 10 km) is frequently performed to analyze compliance with air quality regulations and/or to assess potential public health impacts of new developments or policies. A recent example is the UK Department for Transport (2006) analysis of Heathrow Airport, UK. Its purpose was to evaluate the quality of dispersion models that could be used to analyze possible UK airport developments subject to the ambient air quality regulatory constraints of EU Council Directive 1999/30/EC (1999). Violation of the planned annual average NO_2 ambient air quality standard was a major concern at Heathrow, but — partially on account of dispersion modelling results — the UK Government has since proposed expansion of Heathrow (UK Department for Transport, 2007).

There are a number of widely used operational dispersion models applied in a regulatory or policy analysis context. Examples include ADMS (CERC, 2004; Carruthers et al., 1994, 1999; McHugh et al., 2001); AERMOD (Cimorelli et al., 2004); and LASAT by Janicke Consulting. Other models are listed, for example, on the US Environmental Protection Agency website (US EPA, 2008).

ADMS and AERMOD can be described as Gaussian plume models, while LASAT is a Lagrangian model. All have been widely applied and evaluated against experimental results demonstrating predictions of considerable accuracy (Carruthers et al., 1999; Hanna et al., 2001; McHugh et al., 2001; Perry et al., 2005; Hirtl and Baumann-Stanzer, 2007), but may require runtimes of hours to days.

While direct application of models such as AERMOD may be tractable for policy analyses at specific sites, this is not so for large-scale national or international policy assessments. For example, the authors

* Corresponding author.

Email addresses: srhh2@cam.ac.uk (Steven R. H. Barrett), rb11@cam.ac.uk (Rex E. Britter).

are working on assessing local air quality impacts of airports globally, now and for future growth scenarios (Reynolds et al., 2007). This motivates our development of a rapid approach to estimating long-term average pollutant concentrations.

2. General approach

2.1. Meteorological statistics

As we restrict ourselves to long-term average concentrations, we require long-term meteorological statistics rather than any specific period in time. We assume that this is available as a joint probability density function, $p(\theta, \mathbf{m})$, where θ is the plume direction and \mathbf{m} represents the vector of meteorological variables accounted for in dispersion calculations (wind speed, friction velocity, Monin–Obukhov length, etc.). In practice $p(\theta, \mathbf{m})$ could be sampled by taking a time-series of one or more years of meteorological data at a one hour resolution.

Given some dispersion kernel $\chi_i(\dots)$ for quasi-steady ground-level concentrations at coordinates (X, Y) , the annual mean concentration from all sources is given by

$$\langle \chi(X, Y) \rangle = \sum_{i=1}^N \int \int \int p(\theta, \mathbf{m}, Q_i) Q_i \chi_i(X, Y, \theta, \mathbf{m}) d\theta d\mathbf{m} dQ_i, \quad (1)$$

where there are N sources of strength Q_i and each $\chi_i(\dots)$ is appropriate to the particular source. A similar approach was applied by Martin (1971), while the some of the assumptions implicit in general dispersion modelling approaches have been discussed by Calder (1976).

2.2. Coordinates

The notation used herein is that (X, Y) are receptor coordinates, (x, y) are wind direction aligned coordinates, and θ is the plume direction with $\theta = 0$ corresponding to a southerly wind as shown in Fig. 1. They are related by $x = (X - X_i) \sin \theta + (Y - Y_i) \cos \theta$ and $y = (X - X_i) \cos \theta - (Y - Y_i) \sin \theta$, where (X_i, Y_i) is an appropriate translation for source i .

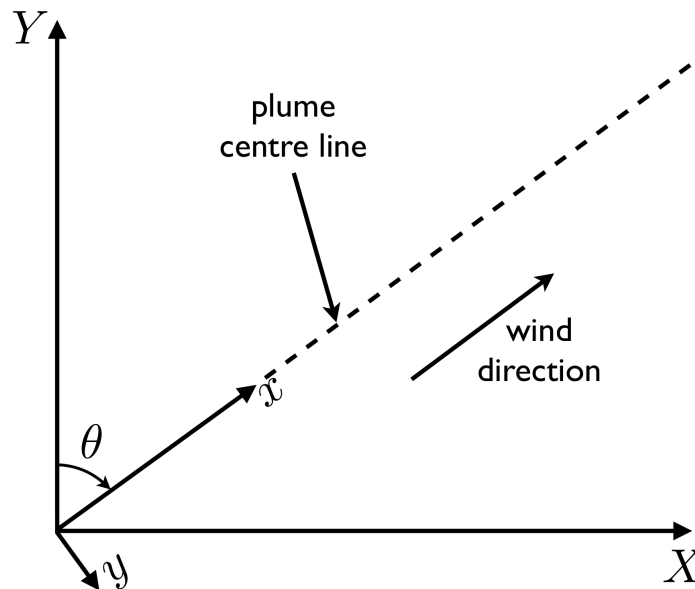


Fig. 1. Schematic of a coordinate systems and plume angle θ (y is defined for convenience so that $x d\theta = dy$).

2.3. Lateral/vertical decoupling

The approach will be to take some $\chi_v(x, z)$ representing vertical dispersion, and impose some $\chi_l(x, y)$ representing lateral dispersion, to produce a final concentration due to a point source of the form

$$\chi(x, y, z)/Q = \chi_v(x, z)\chi_l(x, y), \quad (2)$$

where Q is the emission rate. This is consistent with quasi-analytical approaches to operational dispersion modelling (Pasquill and Smith, 1983).

3. The lateral dispersion averaging approximation

3.1. Derivation

Here we introduce the lateral dispersion averaging approximation (LDAA) to reduce the computation time associated with dispersion calculations. In this we argue that the lateral dispersion profile χ_l has little influence on long-term mean concentrations $\langle \chi \rangle$. LDAA can be applied to any dispersion kernel that can be multiplicatively decomposed into a lateral and vertical component as in Eq. (2).

From Eq. (1) the annual mean concentration due to a point source is given by

$$\langle \chi(X, Y) \rangle = \sum_{i=1}^N \int \int \int p(\theta, \mathbf{m}, Q_i) Q_i \chi_v(x, \mathbf{m}) \chi_l(x, y, \mathbf{m}) d\theta d\mathbf{m} dQ_i, \quad (3)$$

with rotations and translations implicit. It is noted that the integrations and summations can be carried out in any order.

We define a ‘dispersion impact parameter’ as the marginal probability distribution

$$I(\theta, \mathbf{m}) = \int p(\theta, \mathbf{m}, \tilde{Q}) \tilde{Q} d\tilde{Q} \quad (4)$$

such that $\int p(\tilde{Q}) \tilde{Q} d\tilde{Q} = 1$. We also define \bar{Q}_i as the mean emission rate from source i . In this way, a dispersion impact parameter needs to be calculated for each unique temporal emissions profile or site. Conceptually, the dispersion impact parameter quantifies the average impact a source has in each wind direction.

Now, consider some specific receptor at (X_1, Y_1) at which the mean concentration $\langle \chi(X_1, Y_1) \rangle$ is required, where $\theta_1 = \tan^{-1}(X_1/Y_1)$ is the angle that the receptor makes with the Y axis. It is clear that only plume directions near θ_1 contribute significantly to the concentration at (X_1, Y_1) . We therefore assume that $dy \simeq x d\theta$, and that $I(\theta_1, \mathbf{m}) \simeq I(\theta, \mathbf{m})$ across the width of the plume. With these assumptions Eq. (3) then becomes

$$\langle \chi(X, Y) \rangle = \sum_{i=1}^N \bar{Q}_i \int I(\theta, \mathbf{m}) \frac{\chi_v(x, \mathbf{m})}{x} \int \chi_l(x, y, \mathbf{m}) dy d\mathbf{m}, \quad (5)$$

where transformations between (x, y) and (X, Y) coordinate systems are as outlined in section 2.2. Finally by continuity the inner integral is unity, therefore LDAA results in

$$\langle \chi(X, Y) \rangle = \sum_{i=1}^N \bar{Q}_i \int I(\theta, \mathbf{m}) \frac{\chi_v(x, \mathbf{m})}{x} d\mathbf{m}. \quad (6)$$

In most algorithm implementations, an integral sign results in a for-loop. Three nested integrals thus results in three nested for-loops, with the anticipated multiplicative increase in computation time. With the LDAA approach three nested calculations have been reduced to one loop. This may yield significant

computational savings and also shows that long-term mean pollutant concentrations are only weakly influenced by lateral dispersion.

3.2. Pre-smoothing

Computations making use of LDAA will look somewhat jagged due to the lack of smoothing effect offered by the lateral dispersion function χ_l and the discretized wind directions. We propose that a solution is to smooth $I(\theta, \mathbf{m})$ using a weighted mean according to χ_l . This requires the additional assumption that plumes grow approximately linearly for a simplified reference case.

Given this, χ_l can be expressed as a function of θ . Recalling that χ_l is normalized by definition, the smoothed dispersion impact parameter is defined as the convolution

$$\bar{I}(\theta, \mathbf{m}) = I * \chi_l = \int_{-\infty}^{\infty} I(\theta - \tilde{\theta}, \mathbf{m}) \chi_l(\tilde{\theta}, \mathbf{m}) d\tilde{\theta}. \quad (7)$$

It is assumed that $I(\theta, \mathbf{m})$ is represented in a periodic way, i.e. $I(\theta, \mathbf{m}) = I(\theta + 2\pi, \mathbf{m})$ for any θ . In this notation $\chi_l(\tilde{\theta}, \mathbf{m})$ is the value of χ_l at any (x, y) which makes an angle $\tilde{\theta}$ with $y = 0$. Practical calculation can be from

$$\bar{I}(\theta, \mathbf{m}) \simeq \int_{\theta-\pi}^{\theta+\pi} I(\theta - \tilde{\theta}, \mathbf{m}) \chi_l(\tilde{\theta}, \mathbf{m}) d\tilde{\theta}. \quad (8)$$

To show this we consider some lateral dispersion function $\chi_l(x, y, \mathbf{m})$, which grows in width linearly with distance. We define x_n as a normalization distance, such that the χ_l is decreased in height by a factor x/x_n and increased in width by the same factor at distance x , i.e.

$$\chi_l(x, y, \mathbf{m}) = \frac{x_n}{x} \chi_l(x_n, yx_n/x, \mathbf{m}). \quad (9)$$

Note that the integral of χ_l remains unity while its width grows linearly as required. Taking x_n as unity gives

$$\langle \chi(X, Y) \rangle = \sum_{i=1}^N \bar{Q}_i \int \int \chi_v(x, \mathbf{m}) \frac{1}{x} \chi_l(1, y/x, \mathbf{m}) I(\theta, \mathbf{m}) d\theta d\mathbf{m} \quad (10)$$

using the dispersion impact parameter approach. We again consider a specific receptor at (X_1, Y_1) , where $\theta_1 = \tan^{-1}(X_1/Y_1)$. Now assuming that $y/x \simeq \theta_1 - \theta$, we have

$$\langle \chi(X, Y) \rangle = \sum_{i=1}^N \bar{Q}_i \int \frac{\hat{\chi}_v(x, \mathbf{m})}{x} \int \chi_l(1, \theta_1 - \theta, \mathbf{m}) I(\theta, \mathbf{m}) d\theta d\mathbf{m}, \quad (11)$$

which, by definition, reduces to Eq. (6) with the inner integral replaced by $\bar{I}(\theta, \mathbf{m})$ as $I * \chi_l = \chi_l * I$. This could be viewed as an alternative derivation of LDAA, which only requires that most of the plume resides where $\tan^{-1}(y/x) \simeq y/x$ is a good approximation. It does not require that $I(\theta, \mathbf{m})$ changes slowly compared to the width of a plume, but does impose the requirement of linear plume growth with distance. (The smoothed impact parameter can be pre-computed as a function of distance also to relax this restriction.)

3.3. Comparison of LDAA with previous approximations

LDAA, as derived in this paper, can be compared with the ‘narrow plume assumption’ probably described first in an unpublished note by K. L. Calder and F. A. Gifford, 31 Dec. 1969, see Gifford and Hanna (1970); Calder (1976). This was derived rather differently for grids of area sources of considerable extent. It proposed that simply the two-dimensional dispersion kernel be used directly downwind of area sources. Calder (1976) relates this to a point source using an ‘isotropic’ lateral dispersion function. The

key steps were to assume lateral dispersion according to a Dirac delta function and that emissions and meteorology are statistically independent. As such LDAA can be interpreted as a generalization of the narrow plume assumption for the case of long-term averages.

The final result of LDAA is also similar to the sector averaged approach, e.g. as applied in the ASPEN model (US EPA, 2000), in which uniform lateral dispersion is assumed across each sector.

4. Point sources

This section will explore application and implications of LDAA for the simple reference case of a ground-level point source in a neutral boundary layer. This is used to develop a quasi-analytical solution for the annual average pollutant concentration and a scaling law for the area in exceedance of a regulatory limit value.

4.1. Calder-type modelling

Under the simplifying assumption of neutral stability the friction velocity, u_* , is only a function of wind speed, u_r , measured at some reference height, z_r . Thus we define a location-dependent constant:

$$\hat{u} = \frac{u_r}{u_*} = \frac{\ln(z_r/z_0)}{\kappa}, \quad (12)$$

where $\kappa = 0.40$ is the von Kármán constant and z_0 is the roughness length. This is appropriate for neutral conditions (Stull, 1997).

4.1.1. Lateral dispersion

We assume a Gaussian lateral profile of the form

$$\chi_l(x, y) = \frac{1}{\sigma_y \sqrt{2\pi}} \exp\left(-\frac{y^2}{2\sigma_y^2}\right) \quad (13)$$

The standard deviation, σ_y , in Eq. (13) could be based on the concentration weighted plume travel time, however for simplicity we will base it on

$$\sigma_y(x) = bx, \quad (14)$$

valid over short distances. In neutral conditions $b = 0.16$ is appropriate given an assumed urban roughness regime, e.g. Hanna et al. (1982). This linear plume growth is consistent with the restrictions outlined for the smoothed dispersion impact parameter to be valid in its simplest form. It is recognized that in the example results shown the distances exceed linear plume growth, however this is retained for simplicity. Also, to demonstrate the validity of the assumption that $\tan^{-1}(y/x) \simeq y/x$ where plume concentrations are significant, we note that at $y/x = 2b$, 95% of the plume mass is captured and $\tan^{-1}(y/x)$ differs from y/x by 3.2%.

4.1.2. Vertical dispersion

We take the simple solution for a uniform boundary layer that was found by Calder (1952). His formula for (normalized) vertical dispersion reads

$$\chi_v(x, z) = \frac{1}{\kappa u_* x} \exp\left(-\frac{u_r z}{\kappa u_* x}\right), \quad (15)$$

Despite this massive simplification, Calder found good agreement with experiments. Considering only ground-level ($z = 0$) concentrations, the normalized vertical dispersion kernel is

$$\chi_v(x, z) = \frac{\hat{u}}{\kappa x u_r}, \quad (16)$$

where \hat{u} is a constant given by Eq. (12).

4.1.3. Application of LDAA

Equation (16) is strictly for a cross-wind line source. However, we shall interpret it as three dimensional by considering it equal to the cross-wind integrated concentration and imposing a lateral Gaussian profile as in Eq. (2). Indeed, this is consistent with how Calder (1952) compared the theoretical result with experimental results. The annual mean concentration is calculated by application of Eq. (1), i.e.

$$\langle \chi(X, Y) \rangle = \int \int \sum_{i=1}^N \bar{Q}_i p(\theta, u_r) \frac{\hat{u}}{\kappa x u_r} \frac{1}{\sigma_y \sqrt{2\pi}} \exp\left(-\frac{y^2}{2\sigma_y^2}\right) du_r d\theta. \quad (17)$$

Instead, making use of LDAA and the smoothed dispersion impact parameter, the annual mean concentration for a Calder point source is given approximately by

$$\langle \chi(X, Y) \rangle = \sum_{i=1}^N \bar{Q}_i \bar{I}_C(\theta_i) \frac{\hat{u}}{\kappa R_i^2}, \quad (18)$$

where $R_i^2 = (X - X_i)^2 + (Y - Y_i)^2$ and θ_i is the angle that the line joining the source and receptor makes with north. In this case we have aggregated the average inverse wind speed into the dispersion impact parameter so that $I_C(\theta_i) = p(\theta, u_r) \langle u_r^{-1}(\theta) \rangle$, a constant emission rate has been assumed, and \bar{I}_C is I_C smoothed according to Eq. (8). Note that the average inverse wind speed $\langle u_r^{-1}(\theta) \rangle$ sets concentrations. This formulation breaks down at very low wind speeds where along-plume diffusion becomes important. Operational practice often makes use of a minimum wind speed to circumvent this problem (Hanna et al., 1982).

4.2. Exceedance area

The exceedance area is the land area A_r for which the annual mean ground-level concentration exceeds a specified annual mean limit value χ_r . This section will develop an estimate for the exceedance area given the mean species emission rate \bar{Q} and wind statistic $\langle u_r^{-1} \rangle$.

4.2.1. Scaling argument

We use Calder's two-dimensional formula at ground-level, Eq. (16), and assume that all wind directions are equally likely, i.e. $p(\theta) = 1/2\pi$. Correlation between emissions and meteorology is neglected for the scaling law. Since at some distance x from a point source the pollution is spread over $2\pi x$, the annual mean concentration scales as

$$\chi_r \sim \frac{\bar{Q}}{\kappa u_* x \cdot 2\pi x}. \quad (19)$$

This implies that

$$A_r \sim \frac{\bar{Q} \hat{u}}{2\kappa u_r \chi_r}. \quad (20)$$

Further, since we are concerned with an annual average, we define the scaling area as

$$A_r^* = \frac{\bar{Q} \hat{u}}{2\kappa \chi_r} \langle u_r^{-1} \rangle, \quad (21)$$

where $\langle u_r^{-1} \rangle$ is calculated from

$$\langle u_r^{-1} \rangle = \int p(\theta) \langle u_r^{-1}(\theta) \rangle d\theta = \int I_C(\theta) d\theta. \quad (22)$$

4.2.2. Equality of approximate and scaling exceedance areas

The scaling area A_r^* can be shown to equal the exceedance area A_r as calculated by Eq. (18) using the LDAA/dispersion impact parameter approach. For a single point source, Eq. (18) gives the distance from the source to the contour $\langle\chi\rangle = \chi_r$ as

$$x(\theta; \chi_r) = \left(\frac{\bar{Q}\bar{I}(\theta)\hat{u}}{\kappa\chi_r} \right)^{1/2}. \quad (23)$$

The exceedance area is found from

$$A_r = \int_0^{2\pi} \frac{1}{2} x^2(\theta; \chi_r) d\theta, \quad (24)$$

as the area in an arc of angle $\delta\theta$ and radius x is $x^2\delta\theta/2$. Substituting Eq. (23) yields

$$A_r = \frac{\bar{Q}\hat{u}}{2\kappa\chi_r} \int_0^{2\pi} \bar{I}_C(\theta) d\theta \Rightarrow A_r^* = A_r \quad (25)$$

as required. Note that this result is insensitive to use of $\bar{I}_C(\theta)$ or $I_C(\theta)$ as the full angle integral of both should be identical. The key result here is that the total exceedance area, but not its spatial distribution, can be determined by computing only $\langle u_r^{-1} \rangle$. When multiplied by an average population density this provides a first-order measure of the impact of local air pollution on the community.

4.3. Example application

4.3.1. Computational cost

Here we consider the computational cost associated with calculating the ground-level annual average concentration from a ground-level point source for the simple reference case of neutral conditions. We assume that $p(\theta, u_r)$ is available (i.e. a wind rose), or equivalently a one year time-series of hourly (θ, u_r) values. A metric for the computational cost we shall adopt is the number of dispersion kernel evaluations required to determine the annual mean concentration. We define N_{recept} as the number of receptors, and N_{direct} and N_{speeds} as the number of wind directions and wind speed bins in the wind rose input data respectively.

For example, take $N_{\text{recept}} = 40^2$ (a 40×40 grid), $N_{\text{direct}} = 36$ and $N_{\text{speeds}} = 5$. Pre-processing time is not accounted for. If we consider a hourly time-series calculation, this requires $365 \times 24 \times N_{\text{recept}} = 14\,016\,000$ dispersion kernel evaluations. If we instead apply the approach of Eq. (17), i.e. integrating wind rose data, this reduces to $N_{\text{recept}} \times N_{\text{direct}} \times N_{\text{speeds}} = 288\,000$ calculations. Applying LDAA alone results in $N_{\text{recept}} \times N_{\text{direct}} = 57\,600$ calculations, while combining this with the approach making use I_C or \bar{I}_C requires $N_{\text{recept}} = 1600$ dispersion kernel evaluations.

It can be seen that the combined LDAA/dispersion impact parameter approach is more than 10^2 times faster than wind rose integration, and nearly 10^4 times faster than an time-series approach.

4.3.2. Point source NO_x concentrations

To provide a specific example application, we consider NO_x emissions from aircraft on the ground at Heathrow Airport, UK. The total ground-level aircraft NO_x emissions for 2002 totaled 1768 tonnes, corresponding to a mean emission rate of $Q = 0.0561 \text{ kgs}^{-1}$ (Underwood et al., 2004). The meteorological data used is also for 2002.

It is intuitive that time-series and wind rose integration approaches should yield nearly identical concentration fields. We will take the latter as the reference case, which corresponds to Eq. (17). Figure 2 shows point source NO_x concentrations as calculated by integration of wind rose data, using LDAA with a dispersion impact parameter (I_C), and using LDAA with a smoothed dispersion impact parameter (\bar{I}_C).

Examination of Fig. 2 shows that the combined LDAA/dispersion impact parameter approach does indeed reproduce the reference results [from Eq. (17)], but with some jaggedness as expected due to the lack of smoothing effect of lateral plume dispersion. Application of the smoothed dispersion impact parameter recovers the reference results to an accuracy almost visually indistinguishable with the expected relative time saving of approximately two orders of magnitude.

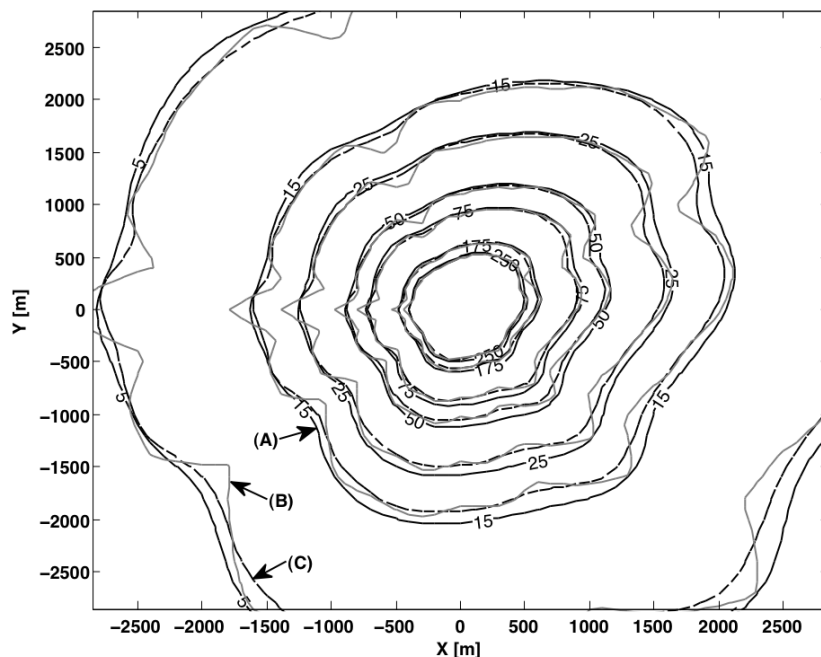


Fig. 2. Annual mean NO_x concentration [μgm^{-3}] from a point source representing Heathrow Airport aircraft sources, as calculated using direct numerical integration of a wind rose (A), LDAA/dispersion impact parameter approach (B), and LDAA/smoothed dispersion impact parameter approach (C).

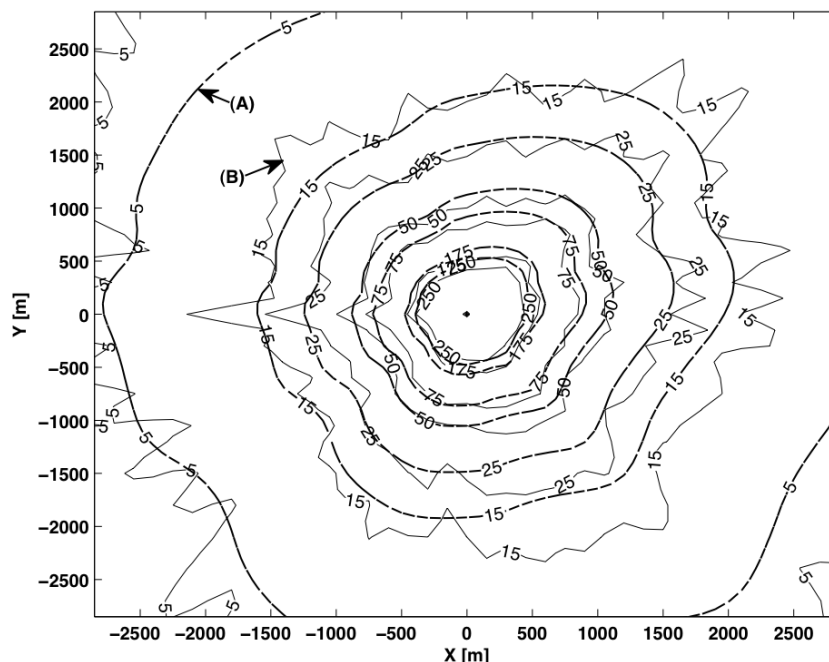


Fig. 3. Annual mean NO_x concentration contours [μgm^{-3}] as calculated by the LDAA/smoothed dispersion impact parameter approach (A) and AERMOD (B) for the Heathrow point source reference case.

Figure 3 shows a comparison between results calculated by AERMOD (accounting for variations in atmospheric stability) and the LDAA/smoothed dispersion impact parameter approach developed from

the simple Calder (1952) formula. Meteorological input data for Heathrow from 2002 was used. The AERMOD runtime was approximately 200 s on an Intel 1.7 GHz personal computer with 2 GB of RAM, as compared to approximately 1 s for the simpler approach.¹ The jaggedness of the AERMOD results can be attributed to the discrete wind angles recorded.

We note that it is not necessarily appropriate to assume neutral conditions in all regions except as a first-order estimate.

4.3.3. Exceedance area

Using the Heathrow example, the exceedance area scaling law (defined in section 4.2) gives $A_r^* = 4.79 \text{ km}^2$ for an arbitrarily chosen limit value of $\chi_r = 50 \mu\text{gm}^{-3}$. This compares with reference value of $A_r = 4.70 \text{ km}^2$ (using direct numerical integration of wind rose data).

Computing A_r from a concentration field calculated by the LDAA/smoothed dispersion impact parameter approach yields results identical to A_r^* to within interpolation errors, numerically demonstrating the earlier result of section 4.2.2 that given some $\langle u_r^{-1} \rangle$, any $p(\theta)$ results in the same total exceedance area.

Specifically, this indicates that LDAA combined with a smoothed dispersion impact parameter introduces a 2% error in exceedance area for this reference case in exchange for two orders of magnitude in computational savings, or four orders of magnitude if compared to a time-series approach.

5. Conclusions and future work

For the calculation of long-term average concentrations we have developed the lateral dispersion averaging approximation (LDAA). This shows that lateral dispersion can be neglected provided that the concentration decay is corrected by a factor 1/distance. This directly yields a significant computational saving, as at each receptor only directly upwind sources need to be considered. A physical interpretation is that, over the long-term, lateral dispersion effects cancel out.

LDAA was applied to a simple reference case of a ground-level point source in a neutral boundary layer. This indicated a 2% error is introduced by LDAA according to an area based metric, in exchange for two orders of magnitude computation time saving (or four orders of magnitude if compared to a time-series approach).

A scaling law for exceedance areas was developed. It was shown that, assuming neutral conditions, the area in exceedance of a particular concentration threshold depends only on the average inverse wind speed, and not on the distribution of wind directions.

Future work will apply LDAA and the dispersion impact parameter approach in a way accounting for variations in atmospheric stability and for line and area sources. One approach being developed entails deriving dispersion impact parameters from existing models such as AERMOD. Combined with the theoretical implication of LDAA that lateral dispersion can be neglected for long-term averages, this may significantly reduce the computation time for line and area sources where computational costs are currently most acute. It may also be possible to develop algorithms to directly calculate dispersion impact parameters from the statistics of meteorological variables. For example, in the simplified case of neutral conditions, ground-level pollutant concentrations are directly proportional to $p(\theta) \langle u_r^{-1}(\theta) \rangle$.

Acknowledgements

The authors are grateful to UK Research Councils NERC and EPSRC for providing funding.

¹ Note that execution times are not directly comparable as the algorithms developed in this paper have been prototyped in an interpreted language.

References

- Calder, K., 1952. Some recent British work on the problems of diffusion in the lower atmosphere. In: Proceedings of the US Tech. Conf. Air Pollution. Vol. 787. McGraw-Hill, New York.
- Calder, K. L., 1976. Multiple-source plume models of urban air pollution — their general structure. *Atmospheric Environment* 11, 403–414.
- Carruthers, D., Holroyd, R., Hunt, J. C. R., Weng, W., Robins, A., Apsley, D., Thomson, D., Smith, F., 1994. UK-ADMS: a new approach to modelling dispersion in the earth's atmospheric boundary layer. *Journal of Wind Engineering & Industrial Aerodynamics* 52, 139–153.
- Carruthers, D., Mckeown, A., Hall, D., Porter, S., 1999. Validation of ADMS against wind tunnel data of dispersion from chemical warehouse fires. *Atmospheric Environment* 33, 1937–1953.
- CERC, 2004. ADMS 3 User Guide. Cambridge Environmental Research Consultants Ltd., UK, version 3.2 Edition.
- Cimorelli, A. J., Perry, S. G., Venkatram, A., Weil, J. C., Paine, R. J., Wilson, R. B., Lee, R. F., Petersand, W. D., Brode, R. W., Paumier, J. O., 2004. AERMOD: description of model formulation (EPA-454/R-03-004). Tech. rep., US Environmental Protection Agency, Office of Air Quality Planning and Standards, Emissions Monitoring and Analysis Division.
- EU Council Directive 1999/30/EC, 1999. Relating to limit values for sulphur dioxide, nitrogen dioxide and oxides of nitrogen, particulate matter and lead in ambient air.
- Gifford, F. A., Hanna, S. R., 1970. Urban air pollution modelling, Paper No ME-320. In: Proceedings of 2nd International Clean Air Congress, Washington, D.C.
- Hanna, S. R., Briggs, G. A., Hosker, Jr., R. P., 1982. Handbook on Atmospheric Diffusion. Technical Information Center, U.S. Department of Energy.
- Hanna, S. R., Egan, B. A., Purdum, J., Wagler, J., 2001. Evaluation of the ADMS, AERMOD, and ISC3 dispersion models with the OPTEX, Duke Forest, Kincaid, Indianapolis and Lovett field datasets. *International Journal of Environment and Pollution* 16 (1–6), 301–314.
- Hirtl, M., Baumann-Stanzer, K., 2007. Evaluation of two dispersion models (ADMS-Roads and LASAT) applied to street canyons in Stockholm, London and Berlin. *Atmospheric Environment* 41, 5959–5971.
- Martin, D. O., 1971. An urban diffusion model for estimating long term average values of air quality. *Journal of the Air Pollution Control Association* 21 (1), 16–19.
- McHugh, C., Carruthers, D., Higson, H., Dyster, S., 2001. Comparison of model evaluation methodologies with application to ADMS 3 and US models. *International Journal of Environment and Pollution* 16 (1–6), 1–11.
- Pasquill, F., Smith, F. B., 1983. Atmospheric Diffusion. Ellis Horwood.
- Perry, S. G., Cimorelli, A. J., Paine, R. J., Brode, R. W., Weil, J. C., Venkatram, A., Wilson, R. B., Lee, R. F., Peters, W. D., 2005. AERMOD: A dispersion model for industrial source applications. Part II: Model performance against 17 field study databases. *Journal of Applied Meteorology* 44 (5), 694–708.
- Reynolds, T. G., Barrett, S., Dray, L., Evans, A., Köehler, M., Schäfer, A., Vera Morales, M., Wadud, Z., Britter, R., Hallam, H., Hunsley, R., 2007. Modelling the environmental & economic impacts of aviation: Introducing the Aviation Integrated Modelling Project. In: 7th AIAA Aviation Technology, Integration and Operations Conference.
- Stull, R. B., 1997. An Introduction to Boundary Layer Meteorology. Kluwer Atmospheric Publishers.
- UK Department for Transport, 2006. Project for the Sustainable Development of Heathrow: Report of the airport air quality technical panels.
- UK Department for Transport, 2007. Adding capacity at heathrow — consultation summary document.

URL <http://www.dft.gov.uk/consultations/open/heathrowconsultation/consultationdocument/>
Underwood, B. Y., Walker, C. T., Peirce, M. J., 2004. Heathrow emission inventory 2002: Part 1. Tech.
Rep. netcen/AEAT/ENV/R/1657/Issue 4, netcen.
US EPA, 2000. User's guide for the assessment system for population exposure nationwide (ASPEN,
version 1.1) model. US Environmental Protection Agency.
US EPA, 2008. EPA Dispersion Modeling website.
URL <http://www.epa.gov/scram001/dispersionindex.htm>